Wind-driven reorganization of coarse clasts on the surface of Mars

Jon D. Pelletier[1]*, Andrew L. Leier[2], James R. Steidtmann[3]
[1]Department of Geosciences, University of Arizona, Gould-Simpson Building, 1040 East Fourth Street, Tucson, Arizona 85721–0077, USA
[2]Department of Geoscience, University of Calgary, Calgary, Alberta T2N 1N4, Canada
[3]Enhanced Oil Recovery Institute, University of Wyoming, Laramie, Wyoming 82071, USA

ABSTRACT

Coarse (pebble to cobble sized) clasts on the intercrater plains of the Mars Exploration Rover *Spirit* landing site exhibit a nonrandom (i.e., uniformly spaced) distribution. This pattern has been attributed to the entrainment and redistribution of coarse clasts during extreme wind events. Here we propose an alternative mechanism readily observable in wind tunnels and numerical models at modest wind speeds. In this process, coarse clasts modify the air flow around them, causing erosion of the underlying substrate on the windward side and deposition on the leeward side until a threshold bed-slope condition is reached, after which the clast rolls into the windward trough. Clasts can migrate across an erodible substrate in repeated cycles of trough formation and clast rolling, "attracting" or "repelling" one another through feedbacks between the local clast density, substrate erosion and/or deposition rate, and substrate elevation. The substrate beneath areas of locally high clast densities aggrades, building up a topographic high that can cause clasts to repel one another to form a more uniform distribution of clasts through time. This self-organized process likely plays a significant role in the evolution of mixed grain size eolian surfaces on Earth and Mars.

INTRODUCTION

Photographs from the Rovers *Spirit* and *Opportunity* have revealed a wealth of detailed information about surface processes on Mars. One of the most enigmatic discoveries documented uniform distributions of coarse (pebble to cobble sized) clasts at the *Spirit* landing site in Gusev Crater (Ward et al., 2005) (Fig. 1). Surficial deposits of this area are composed of impact-ejecta–derived coarse clasts deposited on a wind-eroded sandy substrate (Greeley et al., 2006; Golombek et al., 2006). Ward et al. (2005) used the spacing factor, defined as the ratio of the mean nearest-neighbor spacing to the value expected for a random distribution, to establish that coarse clasts in this area were more uniformly spaced than would be expected for a random distribution. Ward et al. (2005) found uniformly spaced distributions in all areas they studied except for the area near the rim of Bonneville Crater (where the impact-ejecta deposits are especially coarse and recent). Evenly spaced distributions of coarse clasts in eolian deposits on Earth have also been observed and puzzled over for decades (McKee and Tibbits, 1964; Walker and Harms, 1972; Steidtmann, 1974; Schenk, 1990). Ward et al. (2005) hypothesized that the uniform distribution of clasts in Gusev Crater was created as coarse clasts were entrained by the wind during extreme events of a past climate on Mars and reorganized to form a surface of minimum aerodynamic roughness. Entrainment of cobble-sized clasts on Mars, however, requires extremely high wind speeds (i.e., several hundred kilometers per hour) (Ward et al., 2005). It is unclear whether such high wind speeds have occurred on Mars and whether they would, in fact, lead to a more uniform spatial distribution. Laboratory measurements of the aerodynamic roughness of surfaces with a similar density of roughness elements (e.g., clasts) but different spatial distributions (e.g., uniform versus clustered) reveal no significant difference in aerodynamic roughness (Marshall, 1971; Brown et al., 2008), hence it is unclear that the clasts would reorganize to form a more uniform distribution even if they were entrained by the wind.

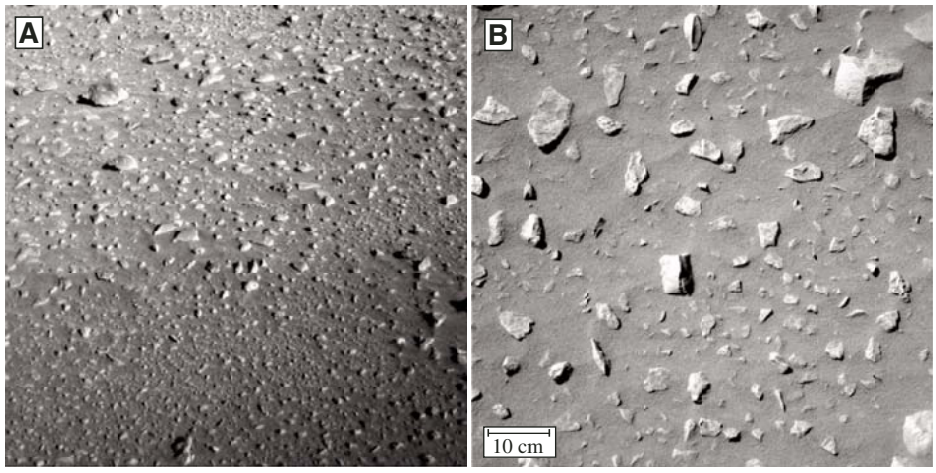

Figure 1. *Spirit* Rover camera images of intercrater plains between Lahontan Crater and Columbia Hills illustrating examples of uniformly spaced clast distributions. A: Portion of Navcam image ID 2 N 137561115 EFF 47 00 P1827 L0 M1. Largest clasts in this image have maximum diameters of ~20 cm. B. Pancam image 2 P 137636467 EFF 47 DQ P2514 R1 C1. After Ward et al. (2005).

Here we propose an alternative explanation motivated by wind tunnel and numerical model experiments. Pebble-sized clasts placed in a wind tunnel atop a sandy substrate undergo transport even at wind speeds much lower than the entrainment threshold of the coarse clasts (Fig. 2). A series of experiments in a wind tunnel of 0.2 m^2 cross-sectional area was performed at room temperature and standard atmospheric pressure to demonstrate this effect. Wind speed in each experiment was increased until just above the saltation threshold for the sand particles (composed of 0.2-mm-mean-diameter,

*E-mail: jdpellet@email.arizona.edu.

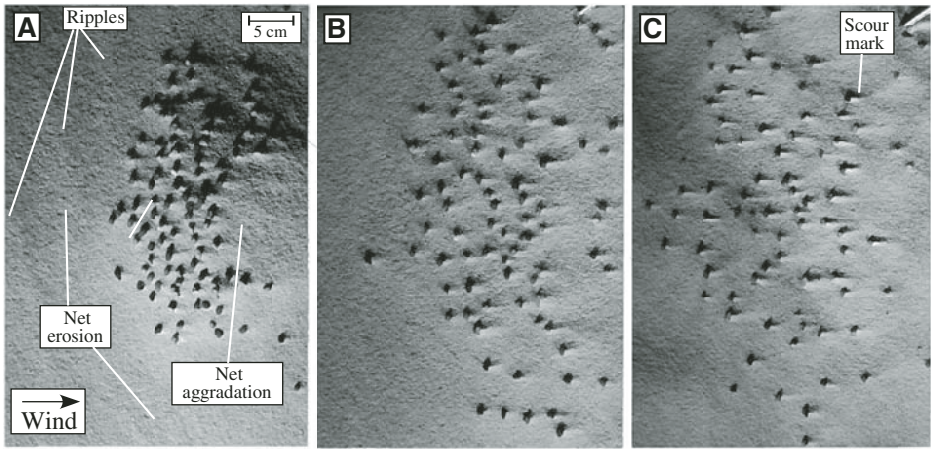

Figure 2. Wind tunnel experiment (conducted by J.R. Steidtmann) illustrating "repulsion" and upwind migration of pebble-sized clasts on wind-erodible sandy substrate. A: Early times of 2 h experiment. B: Intermediate times of 2 h experiment. C: Late times of 2 h experiment.

very well sorted, quartz sand) and was then held fixed for the duration of the experiment. This speed was much lower than the wind speed that would have been necessary to entrain the pebble-sized clasts (1 cm mean diameter). Despite the fact that wind speeds were below the entrainment threshold of the coarse clasts, some of the coarse clasts migrate upwind in the experiments, and the clasts move apart from one another to produce a lower density of clasts over time. Several experiments were run, each lasting ~2 h, with different initial clast configurations. In each case, upwind migration occurred and the final clast density was significantly lower than the original clast density. Ripples with heights and spacings of ~0.5 cm and 10 cm, respectively, formed in areas of low clast density, but their presence did not significantly affect the clast migration process.

Clast migration occurs in the experiments because clasts modify the air flow around them, causing enhanced erosion on the windward side and enhanced deposition on the leeward side to create a wind-aligned scour mark. Scour marks are commonly observed in the field around obstacles in both subaerial and subaqueous flow (Richardson, 1968). Subsequent rolling of the clast into the windward trough causes upwind migration of clasts in the experiment. A similar process has been documented in laboratory flume studies with aqueous flow, i.e., clasts migrate upstream (Fahnestock and Haushild, 1962). Clasts also interact with neighboring clasts via their effects on the boundary layer flow field and the resulting pattern of erosion and deposition. Specifically, regions of higher clast density exert drag on the boundary layer flow, thereby causing local aggradation and increased substrate elevation over time to create relief between areas of higher clast density and areas of lower clast density. Because mass is conserved in this system, deposition in areas of above-average clast density must be balanced by erosion in areas of below-average clast density. Regions of higher clast density undergo aggradation because their wake regions are zones of enhanced deposition, and a larger areal density of wakes leads to a higher local deposition rate. Clasts on the periphery of the zones of high clast density respond to this doming of the underlying substrate by rolling away from the topographic high. This coevolution between local clast density and substrate elevation leads to a more uniform clast density through time in the wind tunnel experiments. These experiments clearly illustrate that clast migration on sandy surfaces does not require clast entrainment by the wind.

NUMERICAL MODEL DESCRIPTION

To further understand this process of clast migration and self-organization, we constructed a numerical model of the coupled evolution of a population of clasts on a wind-erodible substrate. The model is based on Werner's (1995) cellular model of eolian dune development: in the simplest version of Werner's model, a square lattice is established with an initially constant sand thickness. During each time step of the model, a grid point is chosen at random and a unit thickness of sand is removed from the bed. This sand unit is then transported downwind a distance l. At that new location, the sand unit is deposited with a probability p that is <1, unless the new location is within a shadow zone, in which case the particle is deposited with $p = 1$. Shadow zones are defined as portions of the lattice that would be cast in shadow if the surface were illuminated from the upwind direction by a light source angled 15° from the horizontal. Shadow zones approximate the wakes formed on the lee sides of dunes and incipient dunes where deposition is favored. If the sand unit in transport is not deposited at the new location, it is transported downwind by successive jumps of distance l until deposition occurs. Deposition of the sand unit raises the surface elevation of the new location by the unit thickness of sand. If the elevation between any two adjacent points is greater than a certain threshold (i.e., the angle of repose for sand, assumed to be 30° in the model), sand units are transported down the local slope to eliminate the oversteepened condition. Periodic boundary conditions are used, so a sand unit that is transported downwind off the lattice is reintroduced at the other side. The values of p and l control the sand transport rate such that higher values of l and lower values of p lead to higher transport rates. Although aerodynamically simplified, Werner's (1995) model captures the essential feedbacks between the topographic shape and the resulting pattern of erosion and deposition as bedforms evolve through time. Werner's (1995) model is capable of reproducing all of the major dune types and of simulating the interactions between dunes that leads to dune coalescence and breakup.

We modified Werner's (1995) model to include the presence of clasts on the bed, enhanced erosion on the windward side of each clast, and rolling of each clast in response to sloping of the underlying substrate (Fig. 3A). To isolate the effects of clasts on substrate evolution, we applied the shadow zones only to the clasts themselves. Therefore, bedforms do not grow in our model. Enhanced erosion from the windward side of each clast was included by mapping a foreshadow zone where the probability of deposition is 0, thus complementing the shadow zone on the lee side, where the probability of deposition is 1. In areas that are both shadow zones and foreshadow zones, the shadow zone takes precedence (i.e., $p = 1$). The precedence of shadow zones is appropriate because, although obstacles generally cause erosion on the stoss side and deposition on the lee side, the net effect of obstacles is depositional (e.g., King et al., 2005). When the local bed slope beneath the center of each clast exceeds a threshold value given by Φ, the clast rolls downhill until a local slope lower than the threshold value is encountered. The angle of repose or stability for a single clast is given by the equation (Miller and Byrne, 1966)

$$\Phi = \alpha\left(\frac{D}{\overline{K}}\right)^{-\beta}, \quad (1)$$

where D is the clast diameter, $\overline{K}$ is the mean diameter of the particles composing the substrate, α is a parameter incorporating the effects of shape and roundness of the clast and bed particles, and β is a parameter (= ~0.3 in experimental data of Miller and Byrne, 1966) incorporating the effect

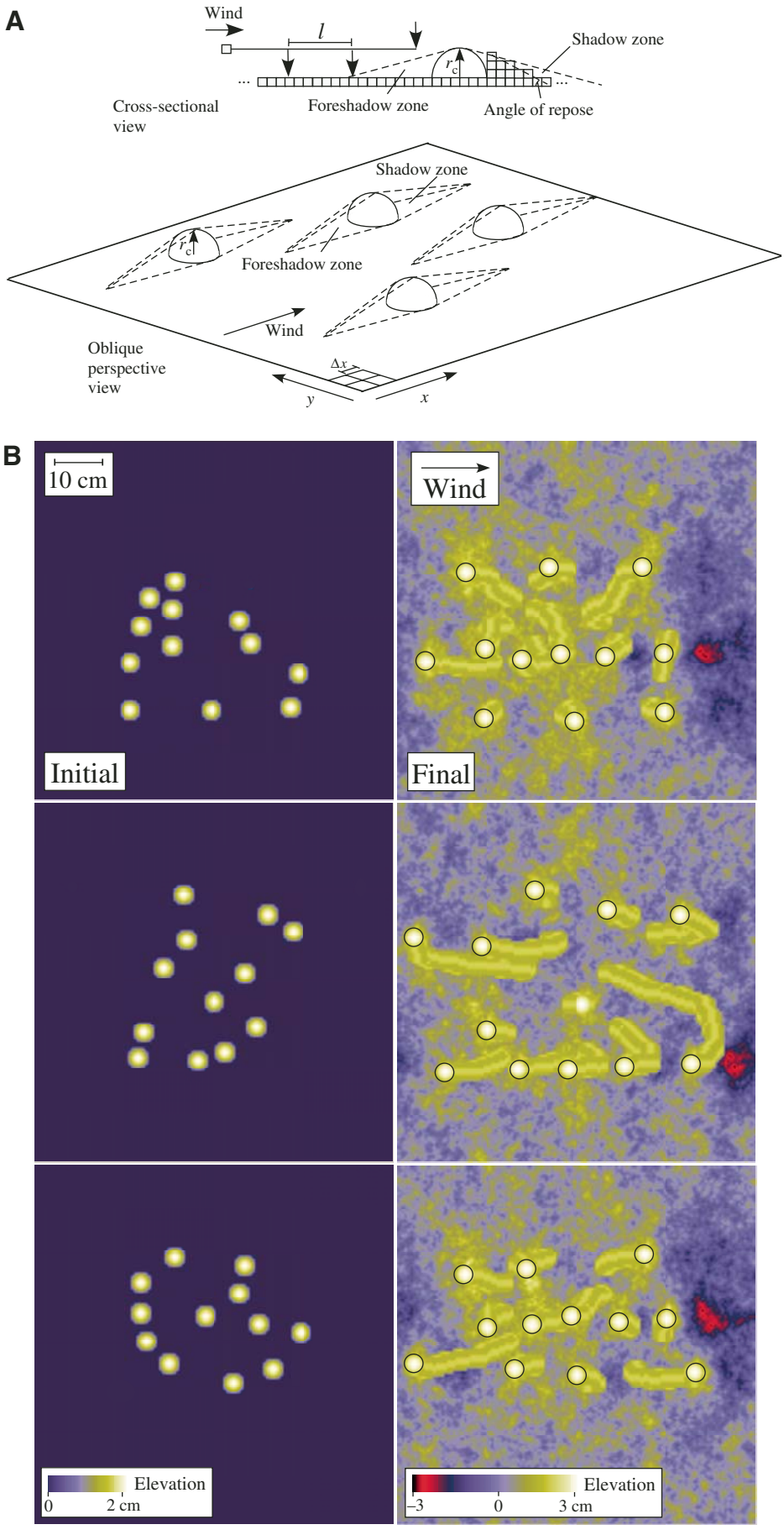

Figure 3. Example numerical model results illustrating clast migration into uniform spatial distribution. A: Schematic diagram of model components. B: Example model results for three initially random configurations of 12 clasts, each 4 cm in diameter, subject to wind from the left. Additional model parameters are *l* = 1 lattice site, probability *p* = 0.2, and threshold bed slope for rolling Φ = 5°.

of sorting of particles on the bed. Equation 1 indicates that the angle of repose becomes small as the ratio of the clast and bed-particle diameters become large. For example, if the granular material is characterized by $\beta = 0.3$ and an angle of repose = 33° for grains of uniform size, the angle of repose will decrease to ~4° if a particle 1000 times larger, but of equivalent shape and roundness, is placed on the bed.

NUMERICAL MODEL RESULTS

In the model results presented here, 12 clasts 4 cm in diameter were initially placed at random within the central portion of the lattice (Fig. 3B, and the animation in the GSA Data Repository[1]). Model results are shown using a jump length $l = 1$ lattice site, probability of deposition $p = 0.2$, and a threshold bed slope for rolling $\Phi = 5°$. Model results are presented using a color map of the elevation of the clast-

[1]GSA Data Repository item 2009013, animation of numerical model illustrating wind-driven reorganization of coarse clasts on an erodible substrate, is available online at www.geosociety.org/pubs/ft2009.htm, or on request from editing@geosociety.org or Documents Secretary, GSA, P.O. Box 9140, Boulder, CO 80301, USA.

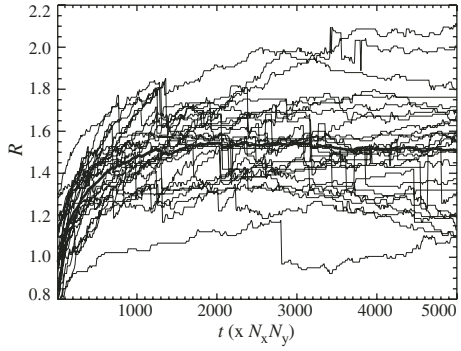

Figure 4. Evolution of spacing factor *R* versus time *t* in model (N_x and N_y are the number of lattice points in the *x* and *y* directions). Plot of spacing factor versus time for 30 (of total of 100) numerical experiments with different initial random clast configurations using same model parameters as in Figure 3B. Spacing factor increases in all runs, from average value (plotted with thick curve) of 1.0 to ~1.5 (of maximum theoretical value of 2.1491).

substrate system after $t = 5000 \times N_x N_y$ time steps have elapsed, where N_x and N_y are the number of lattice points in the x and y directions. In cellular automaton models such as this one it is convenient to report units of time as multiples of the number of grid points, so that results with different grid sizes can be directly compared. Superimposed on the color map of elevation at the final time step is the displacement path of each clast during the model run. In the model runs, erosion from the windward side of each clast and deposition on the leeward side establishes an upwind-oriented bed slope that drives upwind clast migration in multiple episodes of rolling. In fact, if a single clast is placed on the substrate, the model predicts that the clast will migrate precisely upwind. It is important to emphasize that, once a clast rolls into its windward trough, there is a period of time in which the clast will be lower than the surrounding surface and will not move. However, once the trough rolls, it begins the formation of a new trough further upwind, thereby enabling the clast to roll again once the new trough is formed. When a collection of clasts is placed on the substrate, regions of locally high clast density become zones of net aggradation (provided that $p < 0.5$, otherwise they become zones of net erosion), as observed in the wind tunnel experiments. Regions of higher clast density in the model have more shadow zones per unit area, hence aggradation will be favored in those areas. Aggradation of high-clast-density regions causes the local substrate elevation to increase through time, building up relief on the substrate that causes clasts to roll away from regions of higher clast density to regions of lower clast density. This process stops when the spatial variations in erosion and deposition caused by variable clast density are insufficiently large to create local substrate slopes in excess of the threshold value Φ. It should be noted, however, that, if clasts are initially spaced very close to one another, they may not move apart because local deposition may not produce a sufficiently steep slope between the two clasts to force them to move in different directions. For this reason, the initial distribution of clasts, together with the value of Φ, controls the extent of clast reorganization in a complex manner.

In addition to the tendency of clasts to evolve toward lower density, clasts in the model also tend to align parallel to the direction of the wind. The most stable configuration of the surface is one with minimal spatial variations in erosion and deposition. At the scale of individual pairs of clasts, spatial variations are minimized if the foreshadow zone of one clast aligns with the shadow zone of the upwind clast. Reorganization of clasts into equally spaced patterns is a robust feature of the model for a wide range of model parameters l, p (for <0.5), and Φ. The model can be modified to include net erosion of the substrate over time (e.g., by not reintroducing some fraction of sand units transported off the lattice back into the upwind side). In the results of this modified model, clast migration occurs more readily for a given value of Φ because greater relief builds up between the eroding substrate and the nonerodible substrate beneath each clast, eventually triggering the rolling and/or migration of clasts with even large values of Φ.

Changes in the spatial distribution of clasts in the model can be quantified using the spacing factor. The spacing factor provides an objective measure of clast self-organization within a model run and it quantifies the robustness of this process in a set of many runs. In 100 model runs with different initially random clast configurations but constant model parameter values of $l = 1$, $p = 0.2$, and $\Phi = 5°$, the spacing factor in each experiment increased (Fig. 4). On average (shown as thick curve), the spacing factor increases from nearly 1 (the expected spacing factor for randomly distributed clasts) to ~1.5 out of a theoretical maximum value of 2.1491. The mean spacing factor of 1.5 compares favorably with the values observed on Mars that range from 1.2 to 1.7 at the *Spirit* landing site (Ward et al., 2005). These model results illustrate the robustness of the clast self-organization process regardless of the specific initial configuration of clasts.

ACKNOWLEDGMENTS

Pelletier acknowledges partial funding by the Mars Fundamental Research Program, grant NNG05GM30G. We thank Nathan Bridges and an anonymous reviewer for helpful reviews that significantly improved the manuscript.

REFERENCES CITED

Brown, S., Nickling, W.G., and Gillies, J.A., 2008, A wind tunnel examination of shear stress partitioning for an assortment of surface roughness distributions: Journal of Geophysical Research, v. 113, F02S06, doi: 10.1029/2007JF000790.

Fahnestock, R.K., and Haushild, W.L. 1962, Flume studies of the transport of pebbles and cobbles on a sand bed: Geological Society of America Bulletin, v. 73, p. 1431–1436.

Golombek, M.P., and 17 others, 2006, Geology of the Gusev cratered plains from the *Spirit* rover traverse: Journal of Geophysical Research, v. 111, no. E2, E02S07, doi: 10.1029/2005JE002503.

Greeley, R.E., and 21 others, 2006, Gusev crater: Wind-related features and processes observed by the Mars Exploration Rover *Spirit*: Journal of Geophysical Research, v. 111, E02S09, doi: 10.1029/2005JE002491.

King, J., Nickling, W.G., and Gillies, J.A., 2005, Representation of vegetation and other nonerodible elements in aeolian shear stress partitioning models for predicting threshold transport: Journal of Geophysical Research, v. 110, F04015, doi: 10.1029/2004JF000281.

Marshall, J.K., 1971, Drag measurements in roughness arrays of varying density and distribution: Agricultural Meteorology, v. 8, p. 269–292, doi: 10.1016/0002–1571(71)90116–6.

McKee, E.D., and Tibbits, G.C., 1964, Primary structures of a seif dune and associated deposits in Lybia: Journal of Sedimentary Petrology, v. 34, p. 5–17.

Miller, R.L., and Byrne, R.J., 1966, The angle of repose for a single grain of sand on a fixed rough bed: Sedimentology, v. 6, p. 303–314, doi: 10.1111/j.1365–3091.1966.tb01897.x.

Richardson, P.D., 1968, The generation of scour marks near obstacles: Journal of Sedimentary Petrology, v. 38, p. 965–970.

Schenk, C.J., 1990, Processes of eolian sand transport and deposition, *in* Fryberger, S.G., et al., eds., Modern and ancient eolian deposits: Petroleum exploration and production: Denver, Colorado, SEPM (Society for Sedimentary Geology).

Steidtmann, J.R., 1974, Evidence for eolian origin of cross-stratification in sandstone of the Caspar Formation, southwesternmost Laramie Basin, Wyoming: Geological Society of America Bulletin, v. 85, p. 1835–1842.

Walker, T.R., and Harms, J.C., 1972, Eolian origin of flagstone beds, Lyons Sandstone (Permian), type area, Boulder County, Colorado: Mountain Geologist, v. 9, p. 279–288.

Ward, J.G., Arvidson, R.E., and Golombek, M., 2005, The size-frequency and areal distribution of rock clasts at the *Spirit* landing site, Gusev Crater, Mars: Geophysical Research Letters, v. 32, L11203, doi: 10.1029/2005GL022705.

Werner, B.T., 1995, Eolian dunes: Computer simulations and attractor interpretation: Geology, v. 23, p. 1,107–1,110.

Manuscript received 21 April 2008
Revised manuscript received 17 September 2008
Manuscript accepted 19 September 2008

Printed in USA